AUTOMATIC EQUALIZATION FOR IN-CAR COMMUNICATION SYSTEMS

Philipp Bulling[1], *Klaus Linhard*[1], *Arthur Wolf*[1], *Gerhard Schmidt*[2]
[1]*Daimler AG*, [2]*Kiel University*
philipp.bulling@daimler.com

Abstract: An automatic equalization filter for in-car communication (ICC) systems is presented. ICC systems usually use an adaptive filter to stabilize the feedback loop between the loudspeakers and the speaker microphone. In this work, a second adaptive filter is introduced that aims at equalizing the sound, radiated from one or more loudspeakers, at the listener's position in order to achieve a linear frequency response. Therefore, a microphone is placed close to the listener's ears in the car ceiling. To obtain a flat frequency response at the listener's position, the loudspeaker signal must be equalized with the inverse frequency response of the path between the loudspeakers and the microphone. This path is described by the impulse response and it is estimated by means of an adaptive filter in this work. To design the equalization filter, the frequency response of the adaptive filter is used. Target applications are speech applications operating in a closed electro-acoustic loop, such as ICC systems. However, the idea can also be applied to other audio presentations. Both simulations and tests in a real car show that the proposed automatic equalization filter improves speech quality in terms of a natural sounding system.

1 Introduction

When driving at high velocities, communication inside a car becomes difficult due to large background noise levels. An ICC system improves communication by capturing the talker's voice and play it back via loudspeakers close to the listeners. However, this results in a closed electro-acoustic loop, since the microphone not only captures the local speech, but also the feedback from the loudspeakers. This requires elaborate feedback cancellation algorithms. To achieve a high signal-to-noise ratio (SNR) and a high speech input level, despite the background noise, the microphones are located close to the mouths of the talkers. A suitable solution is, for example, mounting the microphones above the seats in the car ceiling. Ideally, to enhance communication between all passengers, every seat has its own microphone. A schematic block diagram of an ICC system is shown in Fig. 1. For convenience, only two microphones are shown. In the figure, the voice of the front left passenger is captured and played back at the rear seat. In the same way, the voice of the rear passengers can be played back at the front seat. Switching between the different channels is realized with a loss control in such a way, that only one channel is active at the same time [1]. For this reason, in the following only one channel is regarded. In a real system, the proposed algorithm is applied to all channels.

The listener perceives a mixture of the direct sound and the loudspeaker signal, both signals convolved with the corresponding impulse response from the sound source to the ears. Especially in large cars, measurements show that the direct sound is damped between 10 dB up to 20 dB at the listeners ears, compared to the loudspeaker signal. The signal radiated from the loudspeakers is colored by the frequency responses of the loudspeakers and the microphone, as well as the acoustic properties of the car cabin. The combination of these effects often causes

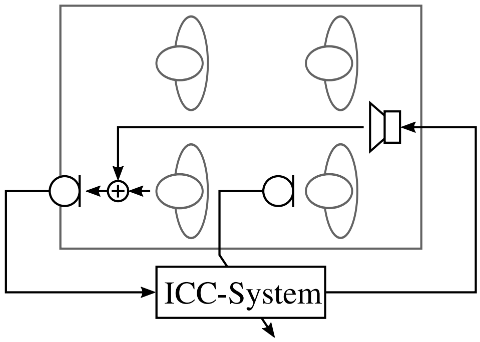

Figure 1 – Schematic block diagram of an ICC system for one talker and one listener. The microphone above the rear-seat is used to adjust the equalization filter.

the speech to sound unnatural. To obtain a natural sounding system, an automatic equalization filter is proposed in this work, that equalizes the sound, radiated from the loudspeakers, at the listener's ears. To adjust the equalizer, the microphone above the listener's seat is used. Therefore, two assumptions are made:

1. The frequency response of the microphone is approximately flat in the frequency range of speech, ranging from 100 Hz to 10.000 Hz. If this is not the case, a filter with a corrected frequency response may be used.

2. The microphone is located close to the listener's ears, such that the impulse response from the loudspeakers to the ears approximately equals the impulse response from the loudspeakers to the microphone.

2 Related Work

Early approaches for ICC systems focus on equalizing the feedback path, i. e. the path from listener loudspeaker to talker microphone. The problem that these filters address, is the electro-acoustic feedback, caused by the closed loop, that limits the stability of such a system. The goal of these approaches is to improve stability by damping the peaks in the frequency response between loudspeaker and microphone. This can either be done by measuring the impulse response in advance and place fixed notch filters at frequencies, where the room's frequency response shows peaks, or by automatic equalization methods based on howling detection [2]. Howling primarily occurs at frequencies, where the stability limit is reached first, i. e. at peaks within the frequency response. If howling is detected, a notch filter is placed at the corresponding frequency to damp the peak. However, this kind of equalization not necessarily improves the sound quality at the listener's position, since the coupling between the listener loudspeaker and the talker microphone is not equal to the path between listener loudspeaker and listener ear.

During the last years, different publications addressed the problem of acoustic feedback cancellation by means of adaptive filters [3]. Here, the main challenge lies in a strong correlation between loudspeaker signal and local speech, that restricts the convergence of the adaptive filter. This problem is addressed for example in [4, 5, 6]. With these approaches, the acoustic feedback can be canceled efficiently, which makes the above mentioned early approaches, used for stabilization, unnecessary.

In this work the focus is on equalizing the loudspeaker signal in such a way, that the transmission of the local speech to the listener is flat. Similar approaches already exist for hands-free systems, as for example presented in [7, 8]. In these patents, the loudspeaker signal is equalized by means of an echo cancellation filter, under the assumption that the near end microphone is close to the listener's ears. The difference in the present work is that in case of acoustic feedback cancellation a second adaptive filter is required to estimate the path between loudspeaker and listener microphone. The proposed algorithm is an extension to the recently published feedback canceler [9]. However, it can also be applied to other feedback cancellation approaches.

3 Adaptive Filters

The ICC system with the two adaptive filters is depicted in Fig. 2. In the figure, n denotes the

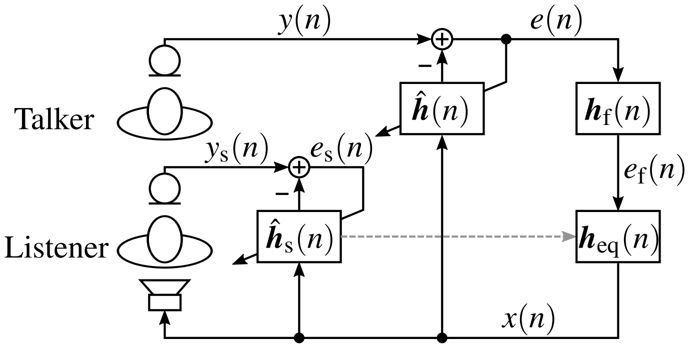

Figure 2 – Schematic block diagram of the adaptive filters, required for both feedback cancellation and automatic equalization.

discrete time index and bold symbols characterize vectors. The adaptive filter $\hat{\boldsymbol{h}}(n)$ estimates the impulse response between loudspeaker signal $x(n)$ and talker microphone $y(n)$. The task of this adaptive filter is to cancel the feedback. In this work, the focus is on the the second adaptive filter $\hat{\boldsymbol{h}}_{\mathrm{s}}(n)$ which estimates the impulse response of the short path, i. e. the path between loudspeaker $x(n)$ and listener microphone $y_{\mathrm{s}}(n)$. The dashed arrow indicates that $\hat{\boldsymbol{h}}_{\mathrm{s}}(n)$ controls the impulse response of the automatic equalization filter $\boldsymbol{h}_{\mathrm{eq}}(n)$. The impulse response of the forward path $\boldsymbol{h}_{\mathrm{f}}(n)$ contains the system gain, adjusted by the user, as well as a delay caused by block processing.

In the figure, all signals are shown in the time-domain. However, to reduce computational complexity, both the adaptive filters as well as the equalizing filter are implemented in the frequency-domain, utilizing fast convolution. The feedback cancellation filter $\hat{\boldsymbol{h}}(n)$ is implemented as described in [9], using a reverb-based stepsize control to improve convergence. The frequency-domain implementation of the adaptive filter $\hat{\boldsymbol{h}}_{\mathrm{s}}(n)$ is described in the following.

As described in Sec. 1, the local speech of the talker $s(n)$ is damped approx. 10 dB to 20 dB at the listener microphone. Hence, at the listener microphone the correlation between local speech and loudspeaker signal is weak, such that the adaptive filter $\hat{\boldsymbol{h}}_{\mathrm{s}}(n)$ converges to the desired solution without the need of further control mechanisms. Therefore, a standard frequency-domain adaptive filter (FDAF), as for example described in [10, 11] can be applied.

Ideally, the FDAF is implemented within an overlap-save filterbank, to avoid errors caused by circular convolution. This is shown in Fig. 3. The signal $s_{y_{\mathrm{s}}}(n)$ represents the direct sound of the local speech, arriving at the listener microphone. The real impulse response of the short path, that has to be estimated, is denoted by $\boldsymbol{h}_{\mathrm{s}}(n)$. In the frequency-domain, $\hat{\boldsymbol{H}}_{\mathrm{s}}(\mu,k)$ is the subband impulse response, obtained by blockwise discrete fourier transform (DFT) of the estimation $\hat{\boldsymbol{h}}_{\mathrm{s}}(n)$. In Fig. 3, the blocks right to the DFT/IDFT blocks symbolize the N time-domain samples that are transfered to the frequency-domain. The frameshift is $L = N/2$. In case of the loudspeaker signal, this results in

$$\boldsymbol{X}(k) = [X(\mu_0,k), X(\mu_1,k), \ldots, X(\mu_{N-1},k)]^T = \mathrm{DFT}\left\{[x(n-N+1), \ldots, x(n)]^T\right\}, \quad (1)$$

where k is the sub-sampled block index ($n = k \cdot L$) and $\mu = \mu_0, \ldots, \mu_{N-1}$ are the discrete frequency bins. To avoid errors caused by circular convolution, the first half of the error signal

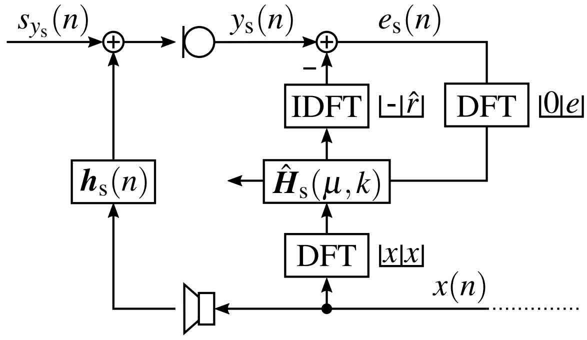

Figure 3 – Schematic block diagram of a frequency-domain adaptive filter, implemented within an overlap-save filterbank.

block must be set to zero before the DFT is applied, i. e.

$$\boldsymbol{E}_s(k) = [E_s(\mu_0,k), E_s(\mu_1,k), \ldots, E_s(\mu_{N-1},k)]^T = \text{DFT}\left\{[\boldsymbol{0}_L, e_s(n-L+1), \ldots, e_s(n)]^T\right\}, \quad (2)$$

where $\boldsymbol{0}_L$ is a zero vector of length L. The filter output $\hat{r}(n)$ is obtained by inverse discrete fourier transform (IDFT) and discarding the first half of the resulting block. With vector $\boldsymbol{X}(\mu,k)$

$$\boldsymbol{X}(\mu,k) = [X(\mu,k), X(\mu,k-1), \ldots, X(\mu,k-M+1)]^T, \quad (3)$$

summarizing the M previous taps of the loudspeaker signal, the update of the adaptive filter can be written as

$$\hat{\boldsymbol{H}}_s(\mu,k+1) = \hat{\boldsymbol{H}}_s(\mu,k) + \alpha(\mu,k) \cdot \frac{E_s(\mu,k) \cdot \boldsymbol{X}^*(\mu,k)}{\|\boldsymbol{X}(\mu,k)\|^2}. \quad (4)$$

In Eq. (4), $\|\cdot\|^2$ is the squared Euclidean norm and $(\cdot)^*$ denotes complex conjugate. Again, due to the circular convolution theorem, the second half of Eq. (4) must be set to zero in the time-domain. The stepsize of the filter update is $\alpha(\mu,k)$. To improve the convergence rate, it is controlled with an approximation of the optimum stepsize

$$\alpha_{\text{opt}}(\mu,k) \approx \alpha(\mu,k) = \alpha_{\text{fix}} \cdot \frac{\overline{|X(\mu,k)|^2}}{\overline{|E_s(\mu,k)|^2}} \cdot \gamma(\mu,k), \qquad \gamma(\mu,k) \approx \overline{\left\|\boldsymbol{H}_s(\mu,k) - \hat{\boldsymbol{H}}_s(\mu,k)\right\|^2} \quad (5)$$

as for example derived in [9], with $\gamma(\mu,k)$ being an estimation of the system distance and $\overline{(\cdot)}$ denoting a smoothed variable. α_{fix} is a constant factor, allowing to adjust the overall stepsize. In this work, it was found that $\alpha_{\text{fix}} = 0.3$ is an appropriate value for the investigated scenarios.

In Fig. 4, a measured impulse response and its corresponding frequency response are shown. The impulse response was measured in a van with three seat rows. The car has four loudspeakers in the passenger compartment, two of them mounted in the car ceiling and two in the side panels left and right. Four microphones are mounted in the car ceiling, one above each front seat and one above each seat of the third seat row. The delay time $T_D = 1.0$ ms is the time it takes for a sound wave, radiated from the closest loudspeaker, to arrive at the microphone. The reverberation time $T_{60} = 101.6$ ms is calculated from the impulse response's energy decay curve (EDC). At around -30 dB the EDC is bent (black line), due to the measurement noise. Therefore, to obtain the T_{60}, the EDC is extrapolated linearly in a logarithmic scale (grey dashed line).

In this work, a sampling frequency of $f_s = 44.1$ kHz is used. The DFT length is $N = 512$ samples, i. e. the frameshift is $L = 256$. To cover the most relevant part of the impulse response shown in Fig. 4, the adaptive filter has $M = 8$ taps. Hence, the length of the estimated impulse response $\hat{\boldsymbol{h}}_s(n)$ is $N_h = M \cdot L = 2048$ samples or 46.4 ms, which approximately corresponds to $T_{60}/2$.

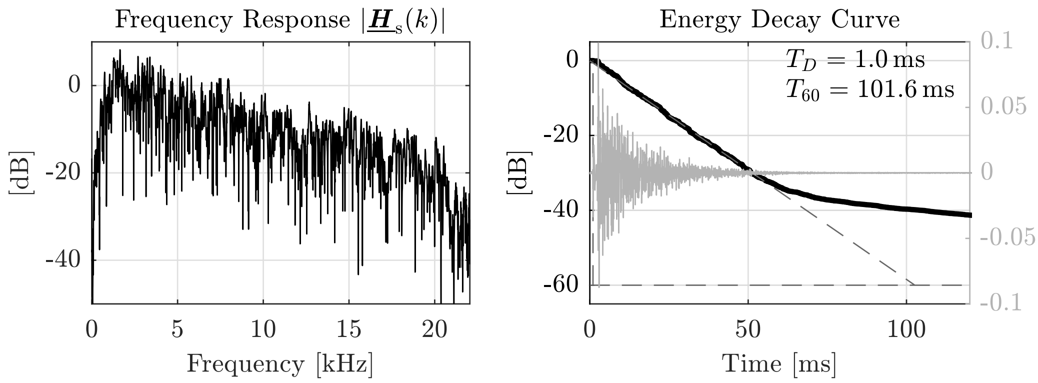

Figure 4 – Frequency response and impulse response from rear the loudspeakers to the microphone rear left.

4 Automatic Equalization

If the loudspeaker signal is equalized with the inverse of the frequency response, shown in Fig. 4, the listener perceives an approximately white spectrum. Hence, the automatic equalization filter $\boldsymbol{h}_{\mathrm{eq}}(n)$ is designed in such a way, that its frequency response is approximately inverse to the frequency response of the estimation $\hat{\boldsymbol{h}}_{\mathrm{s}}(n)$.

The equalization filter $H_{\mathrm{eq}}(\mu,k) \bullet\!\!-\!\!\circ\, \boldsymbol{h}_{\mathrm{eq}}(n)$ is applied in the frequency-domain. Therefore, the spectrum of the feedback canceler's error signal $E_{\mathrm{f}}(\mu,k) \bullet\!\!-\!\!\circ\, e_{\mathrm{f}}(n)$ is multiplied with $H_{\mathrm{eq}}(\mu,k)$ to obtain the loudspeaker spectrum $X(\mu,k)$, i. e.

$$X(\mu,k) = \overline{H_{\mathrm{eq}}(\mu,k)} \cdot E_{\mathrm{f}}(\mu,k), \tag{6}$$

where, $H_{\mathrm{eq}}(\mu,k)$ is smoothed over time with a first order IIR-filter

$$\overline{H_{\mathrm{eq}}(\mu,k+1)} = \beta \cdot \overline{H_{\mathrm{eq}}(\mu,k)} + (1-\beta) \cdot H_{\mathrm{eq}}(\mu,k). \tag{7}$$

Smoothing is necessary in order to prevent sudden filter changes, which would be audible and therefore impair the sound quality. The smoothing constant β is set to 0.9.

In the following, the steps to obtain $H_{\mathrm{eq}}(\mu,k)$ from the adaptive filter are described. First, the estimated impulse response $\hat{\boldsymbol{h}}_{\mathrm{s}}(n)$ is transfered to the frequency-domain via DFT

$$\hat{\underline{\boldsymbol{H}}}_{\mathrm{s}}(k) = \left[\hat{\underline{H}}_{\mathrm{s}}(\mu_0,k), \hat{\underline{H}}_{\mathrm{s}}(\mu_1,k), \ldots, \hat{\underline{H}}_{\mathrm{s}}(\mu_{N_h-1},k)\right]^T = \mathrm{DFT}\left\{\hat{\boldsymbol{h}}_{\mathrm{s}}(n)\right\}. \tag{8}$$

It is important to recognize that the length of $\hat{\boldsymbol{h}}_{\mathrm{s}}(n)$ is N_h, which is longer than the filterbank length N. As a consequence, also the vector $\hat{\underline{\boldsymbol{H}}}_{\mathrm{s}}(k)$ contains N_h frequency samples. To avoid confusion, in the following, variables with high frequency resolution are denoted by an underline $\underline{(\cdot)}$. Next, the magnitude of $\hat{\underline{\boldsymbol{H}}}_{\mathrm{s}}(k)$ is normalized to 0 dB

$$\underline{H}_{\mathrm{norm}}(\mu,k) = \frac{\left|\hat{\underline{H}}_{\mathrm{s}}(\mu,k)\right|}{\max\left\{\left|\hat{\underline{\boldsymbol{H}}}_{\mathrm{s}}(k)\right|\right\}}. \tag{9}$$

$\underline{H}_{\mathrm{norm}}(\mu,k)$ is then limited to a minimum value d. This is necessary, to avoid that notches within the frequency response are emphasized too much by the inversion. Notches will become peaks in the equalizer and large peaks can cause the closed-loop system to become instable, since the maximum stable gain can be exceeded. This limitation is expressed as

$$\underline{H}_{\mathrm{lim}}(\mu,k) = \begin{cases} \underline{H}_{\mathrm{norm}}(\mu,k) & \text{if } \underline{H}_{\mathrm{norm}}(\mu,k) > d \\ d & \text{else.} \end{cases} \tag{10}$$

After that, $\underline{H}_{\text{lim}}(\mu,k)$ is inverted, i. e. $\underline{H}_{\text{inv}}(\mu,k) = \underline{H}_{\text{lim}}^{-1}(\mu,k)$, and normalized by the arithmetic mean in the interval given by $\mu_{\text{s}} = [\mu_{\text{lo}}, \mu_{\text{hi}}]$

$$\underline{H}_{\text{inv,norm}}(\mu,k) = \frac{\underline{H}_{\text{inv}}(\mu,k)}{\frac{1}{N_{\mu_{\text{s}}}} \sum\limits_{\mu=\mu_{\text{lo}}}^{\mu_{\text{hi}}} \underline{H}_{\text{inv}}(\mu,k)}, \tag{11}$$

where $N_{\mu_{\text{s}}} = \mu_{\text{hi}} - \mu_{\text{lo}} + 1$ is the number of frequency bins within the interval μ_{s}. The band-limits are set to $\mu_{\text{lo}} = 5$ and $\mu_{\text{hi}} = 464$, corresponding to a frequency range of approx. 100 Hz to 10.000 Hz. Values outside this frequency range are set to 1.0

$$\underline{H}_{\text{eq}}(\mu,k) = \begin{cases} \underline{H}_{\text{inv,norm}}(\mu,k) & \text{if } \mu_{\text{lo}} \leq \mu \leq \mu_{\text{hi}} \\ 1.0 & \text{else.} \end{cases} \tag{12}$$

To get a smooth shape, $\underline{H}_{\text{eq}}(\mu,k)$ is smoothed with a non-causal FIR filter along the frequency axis, resulting in $\overline{\underline{H}_{\text{eq}}(\mu,k)}$. By doing so, narrow notches and peaks are broadened and flattened. Finally, to obtain the required filter $H_{\text{eq}}(\mu,k)$ for Eq. (6), the frequencies of $\overline{\underline{H}_{\text{eq}}(\mu,k)}$ have to be subsampled by factor $M/2$. Depending on the utilized filterbank type, projections are necessary to avoid circular convolution.

5 Results

The results of the proposed algorithm are given by means of simulations. For simulations, the impulse responses, measured in the car described in Sec. 3, are used. The short path $\boldsymbol{h}_{\text{s}}(n)$ is modeled with the impulse response given in Fig. 4. The feedback is simulated with the impulse response from the rear loudspeakers to the driver's microphone. The local speech is a male speaker located on the driver seat, recorded at 100 km/h. This results in a SNR of 2.3 dBA at the driver microphone and a SNR of -15.2 dBA at the microphone rear left. Without feedback cancellation or any other algorithm, the system is stable up to 0 dB system gain. Since in the simulations the feedback canceler is active, the gain is set to +10 dB. The simulation time is approx. 19 s.

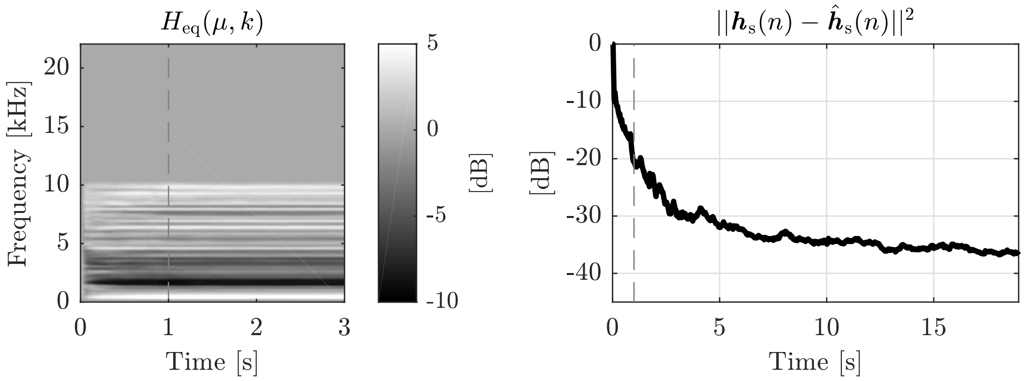

Figure 5 – The spectrogram of $H_{\text{eq}}(\mu,k)$ and the convergence characteristic of the adaptive filter.

The left plot of Fig. 5 shows the temporal progress of the filter coefficients $H_{\text{eq}}(\mu,k)$ as a spectrogram. One can see, that during the first second, the coefficients change. The reason is the convergence characteristic of the adaptive filter, which is shown in the right plot. After 1 s (dashed vertical line), the adaptive filter reaches a system distance of approx. -20 dB. From this point, the coefficients change only slightly.

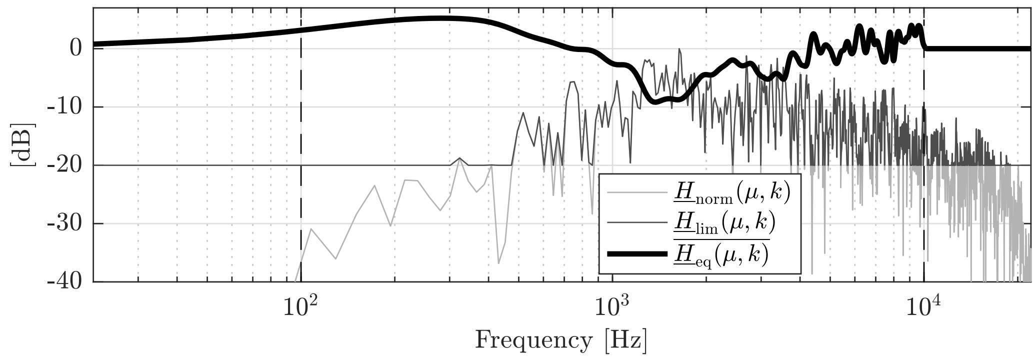

Figure 6 – The frequency response of the automatic equalization filter. For better visualization of the relevant frequencies, a logarithmic scale is used.

The frequency responses of Eqs. (9) and (10) are shown in Fig. 6 together with $\overline{\underline{H}_{\mathrm{eq}}(\mu,k)}$. To create the plot, the adaptive filter's estimation after 19 s simulation time is used. The frequency response is limited to $d = -20\,\mathrm{dB}$.

To evaluate the linearity of the proposed equalization algorithm, the real frequency response $\underline{\boldsymbol{H}}_{\mathrm{s}}(k)$ and the frequency response, weighted with the equalization filter

$$\underline{H}_{\mathrm{filt}}(\mu,k) = \underline{H}_{\mathrm{s}}(\mu,k) \cdot \overline{\underline{H}_{\mathrm{eq}}(\mu,k)}, \tag{13}$$

are compared. Both frequency responses are shown in Fig. 7. A flat frequency response is

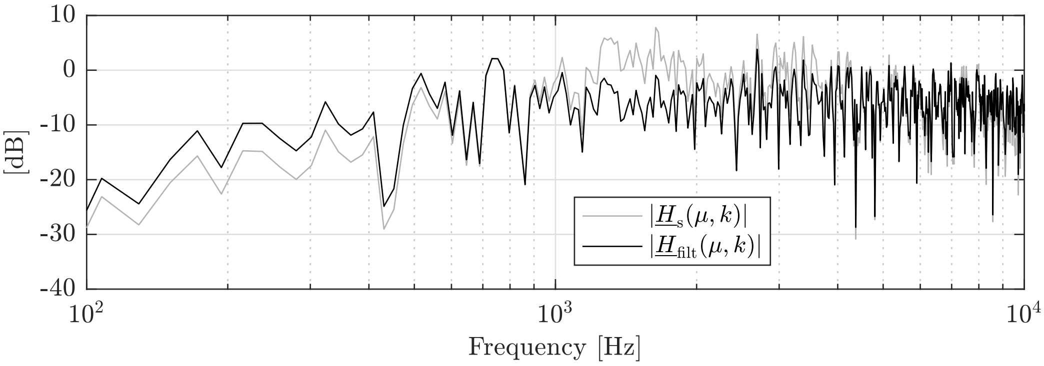

Figure 7 – The frequency response before and after weighting with the automatic equalization filter.

assumed to be ideal. Thus, the squared errors between the frequency responses and their arithmetic mean in the interval $\mu_{\mathrm{s}} = [\mu_{\mathrm{lo}}, \mu_{\mathrm{hi}}]$ are calculated after 19 s simulation time. This results in the distances $D_{\mathrm{s}}(k)$ and $D_{\mathrm{filt}}(k)$

$$D_{\mathrm{s}}(k) = \frac{1}{N_{\mu_{\mathrm{s}}}} \sum_{\mu=\mu_{\mathrm{lo}}}^{\mu_{\mathrm{hi}}} \left(|\underline{H}_{\mathrm{s}}(\mu,k)| - \frac{1}{N_{\mu_{\mathrm{s}}}} \sum_{\mu=\mu_{\mathrm{lo}}}^{\mu_{\mathrm{hi}}} |\underline{H}_{\mathrm{s}}(\mu,k)| \right)^2 \approx \text{-7.45}\,\mathrm{dB}, \tag{14}$$

$$D_{\mathrm{filt}}(k) = \frac{1}{N_{\mu_{\mathrm{s}}}} \sum_{\mu=\mu_{\mathrm{lo}}}^{\mu_{\mathrm{hi}}} \left(|\underline{H}_{\mathrm{filt}}(\mu,k)| - \frac{1}{N_{\mu_{\mathrm{s}}}} \sum_{\mu=\mu_{\mathrm{lo}}}^{\mu_{\mathrm{hi}}} |\underline{H}_{\mathrm{filt}}(\mu,k)| \right)^2 \approx \text{-12.05}\,\mathrm{dB}. \tag{15}$$

For the given scenario, the squared distance $D_{\mathrm{filt}}(k)$ after equalization is approx. 4.6 dB less, than without equalizing. Similar results are also obtained for different impulse responses. Subjective hearing impressions confirm the result. The speech arriving at the listener's ears sounds much more natural if it is processed with the automatic equalization filter.

6 Conclusion and Outlook

An automatic equalization filter for closed-loop electro acoustic systems with adaptive feedback cancellation algorithms was presented. The equalizer aims to achieve a desired frequency response, which is flat over the frequency range of speech. Both simulations and subjective listening showed that the algorithm is capable of flattening the frequency response at the listener's ear.

Further improvements could be controlling the desired frequency response in such a way that it is not white but it depends on the background noise. By doing so, speech intelligibility can be improved, since frequency bands with large background noise power are emphasized. Furthermore, the described equalizer can also be used to improve stability of the closed-loop system. Therefore the resonance frequencies within the estimated impulse response of the feedback cancellation filter must be damped by the equalizer, since these frequencies are very critical for stability. A similar filter design method, as the one described in this work, can be applied.

References

[1] SCHMIDT, G. and T. HAULICK: *Signal processing for in-car communication systems*. In E. HÄNSLER and G. SCHMIDT (eds.), *Topics in Acoustic Echo and Noise Control*, chap. 14, pp. 437–493. Springer, Berlin, 2006.

[2] WATERSHOOT, T. V. and M. MOONEN: *Comparative evaluation of howling detection criteria in notch-filter-based howling suppression*. In *126th Convention of the Audio Engineering Society*. Munich, Germany, 2009.

[3] ORTEGA, A., E. LLEIDA, and E. MASGRAU: *Speech reinforcement system for car cabin communications*. *IEEE Transactions on Speech and Audio Processing*, 13(5), pp. 917–929, 2005.

[4] WITHOPF, J. and G. SCHMIDT: *Estimation of time-variant acoustic feedback paths in in-car communication systems*. In *14th International Workshop on Acoustic Signal Enhancement (IWAENC)*. Antibes, Frankreich, 2014.

[5] BULLING, P., K. LINHARD, A. WOLF, and G. SCHMIDT: *Acoustic feedback compensation with reverb-based stepsize control for in-car communication systems*. In *12th ITG Conference on Speech Communication*. Paderborn, Germany, 2016.

[6] BULLING, P., K. LINHARD, A. WOLF, and G. SCHMIDT: *Approximation of the optimum stepsize for acoustic feedback cancellation based on the detection of reverberant signal periods*. In *43. Deutsche Jahrestagung für Akustik (DAGA)*. Kiel, Germany, 2017.

[7] SCHMIDT, G., T. HAULICK, and M. BUCK: *Equalization in acoustic signal processing*. 2007. European Patent Application EP 1 858 295 A1.

[8] HAULICK, T., G. SCHMIDT, and M. BUCK: *System for equalizing an acoustic signal*. 2012. United States Patent US 8,098,848 B2.

[9] BULLING, P., K. LINHARD, A. WOLF, and G. SCHMIDT: *Stepsize control for acoustic feedback cancellation based on the detection of reverberant signal periods and the estimated system distance*. In *Conference of the International Speech Communication Association (INTERSPEECH)*. Stockholm, Sweden, 2017.

[10] SHYNK, J. J.: *Frequency-domain and multirate adaptive filtering*. *IEEE Signal Processing Magazine*, 9(1), pp. 14–37, 1992.

[11] SOO, J.-S. and K. K. PANG: *Multidelay block frequency domain adaptive filter*. *IEEE Transactions on Acoustics, Speech, and Signal Processing*, 38(2), pp. 373–376, 1990.